Kinetics and Equilibria of the Interaction of Indium(III) with Pyrocathecol Violet by Relaxation Spectrometry

A. Ricciu, F. Secco,* and M. Venturini

Dipartimento di Chimica e Chimica Industriale della Università di Pisa, Via Risorgimento, 35, 56126 Pisa, Italy

B. Garcia and J. M. Leal

Departamento de Quìmica, Laboratorio de Quìmica Fìsica. Universidad de Burgos, 09001 Burgos, Spain

Received: February 29, 2000; In Final Form: May 8, 2000

A temperature-jump apparatus with laser light sources was used to investigate the binding mechanism of indium(III) to pyrocathecol violet (3,3′,4′- trihydroxyfuchsone-2-sulfonic acid, whose neutral form is denoted as H_4L). Spectrophotometric measurements revealed that for $[H^+] > 0.015$ M, the main bound species are MH_3L^{2+} and MH_2L^+ whereas for $[H^+] < 0.015$ M, the main bound species is M_2L^{2+}. Two relaxation effects were observed. The fast relaxation is associated mainly with the reaction steps $M^{3+} + H_3L^- \leftrightarrow MH_3L^{2+}$ ($k_2 = 1.2 \times 10^6$ M^{-1} s^{-1}, $k_{-2} = 1.5 \times 10^5$ s^{-1}) and $MOH^{2+} + H_3L^- \leftrightarrow MH_2L^+$ ($k_3 = 4.4 \times 10^7$ M^{-1} s^{-1}, $k_{-3} = 7.4 \times 10^2$ s^{-1}). The rate constant k_2 decreases, whereas k_{-2} increases, with increasing ionic strength. Addition of Na_2SO_4 results in a large reduction of the fast relaxation time that is ascribed to the binding of indium(III) to sulfate. Analysis of the relaxation time dependence on the sulfate concentration provides the binding constant of the indium−sulfate complex ($K = 1.5 \times 10^2$ M^{-1}). The activation parameters for the step $M^{3+} + H_3L^- \leftrightarrow MH_3L^{2+}$ were obtained as $\Delta H_{1f}^{\ddagger} = 25.3$ kJ mol^{-1}, $\Delta S_{1f}^{\ddagger} = -6.2$ J mol^{-1} K^{-1}, $\Delta H_{1d}^{\ddagger} = 13.4$ kJ mol^{-1}, $\Delta S_{1d}^{\ddagger} = -57$ J mol^{-1} K^{-1}. The enthalpy change of the just described reaction step was measured by spectrophotometry at different temperatures and by the relaxation amplitudes, the average value being $\Delta H_1^0 = 11.9$ kJ mol^{-1}. The slow effect is associated with a complexation path leading to formation of M_2L^+. The amplitude analysis of the slow relaxation gives $\Delta H_2^0 = 7.6$ kJ mol^{-1}. A comparison of this work with other studies on complexation with indium(III) suggests that $In(OH)^{2+}$ reacts according to the I_d mechanism, whereas the mode of activation of $In(H_2O)_6^{3+}$ seems to be less definite because a clear indication about the dependence (or independence) of the rates on the ligand basicity does not emerge. This observation and the slightly negative value of $\Delta S_{1f}^{\ddagger}$ hints at the possibility that indium(III) undergoes complexation by a concerted mechanism.

Introduction

Gallium and indium, in the form of radionuclides, have useful applications in nuclear medicine.[1] Not only do they exhibit unusual affinities for specific types of lesions, such as malignancies and inflammatory processes, they also can be used very effectively as radiolabels for many radiopharmaceutical agents that, in turn, could be used to monitor the functional status of normal organs and their diseases. To localize tumors, Ga^{67} and In^{111} are administrated in the form of complexes (citrate and bleomycin being the most used ligands). These complexes then interact with transferrin, and the hypothesis has been made that the resulting transferrin complex takes the role of the biodistributor of the radiochemicals. It is important to determine what processes are involved in the uptake of gallium and indium complexes by malignant and inflammatory lesions because an understanding of these processes could lead to the identification and design of better radiopharmaceuticals. On the other hand, the study of the behavior of these tervalent metal ions is of interest in itself because the mechanisms of their complex formation reactions present several still obscure aspects; that is, the extensive hydrolysis and polymerization of the metal ions complicate the equilibria to be investigated.[2] Moreover, for ligands of weak acids, the "proton ambiguity" introduces further difficulty in the identification of the reaction paths,[3] as we have experienced in previous investigations of complex formation with tervalent metal ions.[4−7] Finally, focusing on In(III), the assignment of its complexation mechanism is troublesome because the rate of the water exchange process is difficult to measure[8] and the value of its activation volume is not yet available.

We report here on a study of the kinetics and equilibria of the In(III)−pyrocathecol violet system performed by a low-noise T-jump apparatus equipped with lasers as light sources. Pyrocatechol violet was chosen because it was already used as a ligand in a previous investigation[4] of complex formation with Ga(III). Moreover, pyrocatechol violet is one of the organic reagents recommended for spectrophotometric and extraction-photometric determination of tervalent metal ions of the group IIIA. Finally, pyrocatechol violet could be advantageous in ternary systems of the metal−dye−surfactant type, which display enhanced analytical potentialities toward metal extraction and determination.[9]

Experimental Section

Chemicals. All chemicals were analytical grade. Twice-distilled water was used to prepare the solutions and as a reaction

* To whom correspondence should be addressed.

10.1021/jp0007540 CCC: $19.00
Published on Web 07/11/2000

TABLE 1: Reaction Parameters for the Indium(III)−Pyrocathecol Violet System at $I = 0.2$ M and $T = 25$ °C

parameter	value	parameter	value	parameter	value
pK_{A1}[a]	0.14	K_{MH3L}	$(1.2 \pm 0.2) \times 10$ M^{-1}	$k_{-1}K_{C1}^{-1}$	$(1.9 \pm 1.4) \times 10^5$ M^{-1} s^{-1}
pK_{A2}[b]	7.8	K_{MH2L}	$(5.9 \pm 0.1) \times 10^4$ M^{-1}	k_{-2}	$(1.5 \pm 0.1) \times 10^5$ s^{-1}
pK_{A3}[b]	9.8	K'_{M2L}	$(11.2 \pm 0.4) \times 10^{-4}$ M	k_{-3}	$(7.4 \pm 1.1) \times 10^2$ s^{-1}
pK_{A4}[b]	12	k_1	$(1.6 \pm 1.2) \times 10^6$ M^{-1} s^{-1}	$k_{-4}K_{D4}^{-1}$	$(2.0 \pm 0.02) \times 10^5$ M^{-1} s^{-1}
pK_{C2}	0.72	k_2	$(1.2 \pm 0.1) \times 10^6$ M^{-1} s^{-1}		
pK_{OH1}[c]	4.42	k_3	$(4.4 \pm 0.6) \times 10^7$ M^{-1} s^{-1}		
$pK_{M_3(OH)_4}$[c]	9.29	k_4K_{C3}	$(2.1 \pm 0.1) \times 10$ s^{-1}		

[a] Reference 4. [b] Reference 23. [c] Reference 2.

medium. Indium perchlorate was prepared by dissolution of a known weight of the pure metal in a known excess of perchloric acid. The concentration of In(III) was checked by titrating with EDTA as previously described[5] and it was found to coincide with that calculated from the weight of the dissolved metal. Pyrocathecol violet (3,3′,4′-trihydroxyfuchsone-2-sulfonic acid), which shall hereafter be denoted PCV, was from Erba RP and its purity was checked by thin-layer chromatography. Stock solutions of PCV were prepared weekly. Perchloric acid and perchlorates were used to obtain, respectively, the desired acidity and ionic strength.

Methods. The hydrogen ion concentrations of solutions with $[H^+] \leq 0.01$ M where determined by pH measurements performed with a PHM 84 Radiometer Copenhagen instrument. A combined glass electrode was used after replacing the usual KCl bridge by 3 M NaCl to avoid precipitation of $KClO_4$. The electrode was calibrated against sodium perchlorate−perchloric acid solutions of known concentration and ionic strength to give directly $-\log[H^+]$. Spectrophotometric titrations were performed on a Perkin-Elmer lambda 17 double-beam spectrophotometer. Increasing amounts of indium perchlorate were added with a microsyringe to a solution of the ligand that was already thermostated in the spectrophotometric cell. The temperature fluctuactions were within ±0.1 °C throughout. The acidity and ionic strength were kept constant at the desired value during each titration. The data were evaluated by nonlinear least-squares procedures.

Chemical relaxation experiments were performed with a Messanlagen mbh temperature-jump instrument in which, to improve the signal-to-noise ratio, the detection system was replaced by a spectrophotometric device that makes use of lasers as light sources.[10] The signals were detected with a Tektronix TDS 210 oscilloscope, equipped with a digital storage unit capable of memorizing 2500 data points at a maximum sampling rate of 20 MHz, and then transferred to a personal computer and evaluated according to a procedure developed by Provencher.[11] The relaxation times and amplitudes used in this work were averages of at least four repeated experiments, the spread being within 10%. The PCV concentration was changed between 2 and 8×10^{-5} M, whereas the metal concentration was at least 10 times as higher.

Results

Equilibria. PCV, shown in its fully protonated form (H_4L) in Figure 1, is a tetraprotic acid whose dissociation constants are reported in Table 1. The yellow anion H_3L^-, prevailing between pH 2 and 7, exhibits an absorption maximum at 440 nm (Figure 2a), whereas the red form H_4L, present below pH 2, absorbs mainly between 510 and 560 nm. When indium perchlorate is added to a solution of PCV, a sudden change of color indicates the formation of complexes. The shoulder between 500 and 600 nm shown in Figure 2b is ascribed to the formation of a 1:1 complex. On further metal ion addition, a

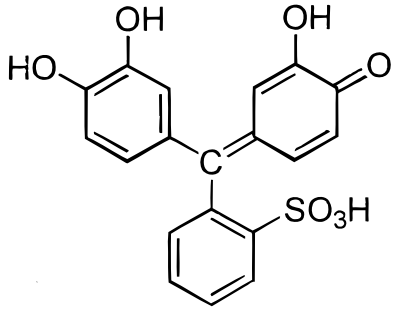

Figure 1. Pyrocathecol violet (3,3′,4′-trihydroxyfuchsone-2-sulfonic acid) structure.

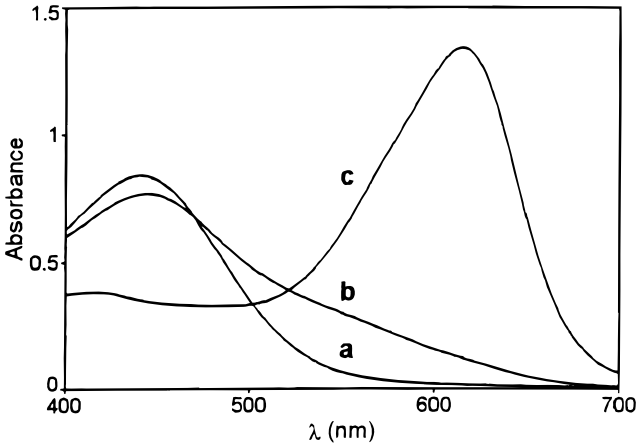

Figure 2. Spectra of the indium(III)-PCV system at pH = 3.0, I = 0.2 M, and T = 25 °C: (a) 8×10^{-5} M PCV; (b) 8×10^{-5} M PCV + 8×10^{-5} M $In(ClO_4)_3$; and (c) 8×10^{-5} M PCV + 2×10^{-3} M $In(ClO_4)_3$.

broad band with maximum at 610 nm appears (Figure 2c), which is ascribed to formation of a dinuclear complex. The reaction is strongly affected by pH. At pH = 0, no evidence of complex formation is obtained, but increasing of the pH causes first the formation of the 1:1 and then of the 2:1 complex, which prevails at pH = 3. Our experiments were carried out in the presence of metal excess ($C_M \gg C_L$). Under these circumstances, formation of the complexes ML_2 and ML_3 should be excluded. At constant acidity, the system is properly represented by the following apparent reactions:

$$M_f + L_f \rightleftharpoons ML_T \quad (1)$$

$$ML_T + M_f \rightleftharpoons M_2L_T \quad (2)$$

where $[L_f] = [H_3L] + [H_4L]$ and $[M_f] = [M^{3+}] + [MOH^{2+}] + 3[M_3(OH)_4^{5+}]$, and where $[ML]_T$ and $[M_2L]_T$ indicate, respectively, the sum of all mononuclear and dinuclear complexes. The equilibrium constants K_{1app} and K_{2app} of reactions 1 and 2 were evaluated with spectrophotometric titrations using the

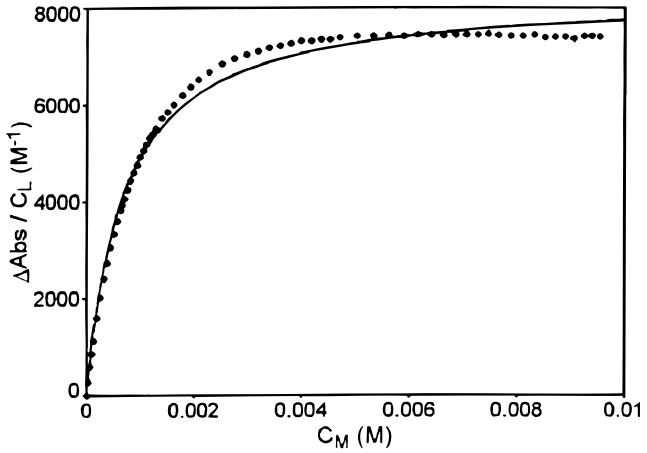

Figure 3. Spectrophotometric titration of the indium(III)-PCV system at $[H^+] = 0.0025$ M, $I = 0.2$ M, and $T = 25$ °C. The continuous line, deviating from experiment, was calculated neglecting the formation of the dinuclear complex.

SCHEME 1: Complex formation reaction scheme.

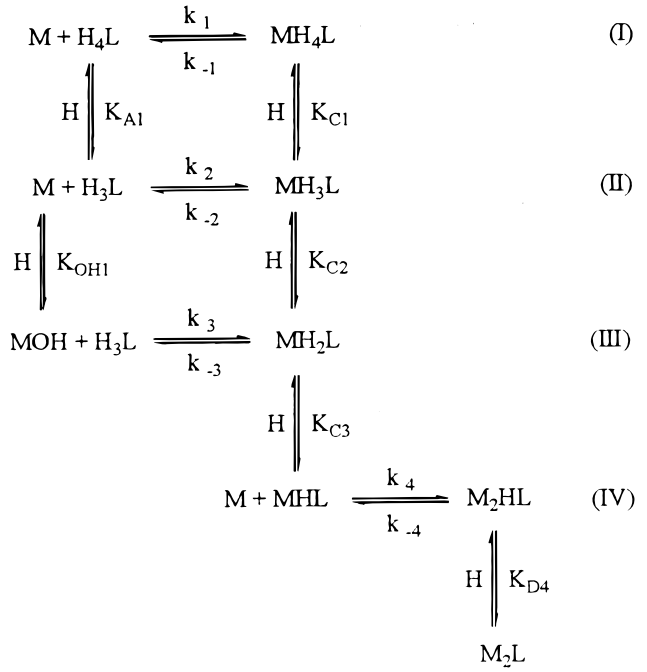

following relationship:

$$\frac{\Delta A}{C_L} = l\left(\frac{\Delta\epsilon_1 K_{1app} C_M + \Delta\epsilon_2 K_{1app} K_{2app} C_M^2}{1 + K_{1app} C_M + K_{1app} K_{2app} C_M^2}\right) \qquad (3)$$

where l is the optical path length, $\Delta A = A - \varepsilon_L C_L$ is the change of absorbance, and $\Delta\varepsilon_1 = \varepsilon_{ML} - \varepsilon_L$ and $\Delta\varepsilon_2 = \varepsilon_{M2L} - \varepsilon_L$ are differences of extinction coefficients. Note that the molar extinction coefficients ε_L, ε_{ML}, and ε_{M2L} are apparent quantities that in principle depend on pH.[5] Figure 3 shows a titration curve where the continuous line deviating from experiment was calculated by neglecting the terms proportional to C_M^2 in eq 3 (i.e., neglecting the formation of the 2:1 complex). These deviations become smaller and smaller as the acidity level is increased, until they disappear for $[H^+] \geq 0.015$ M, where only the mononuclear complex is formed.

Both the spectrophotometric and the kinetic experiments suggest the reaction paths shown in Scheme 1.

The Mononuclear Complex. Analysis of the acidity dependence of the apparent equilibrium constant, K_{1app}, leads to the following relationship:

$$\frac{K_{1app}}{\alpha\beta} = K_{MH_3L} + \frac{K_{MH_2L} K_{OH_1}}{[H^+]} \qquad (4)$$

where K_{MH3L} and K_{MH2L} are, respectively, the equilibrium constants of steps II and III of the reaction scheme. The fractions of the reactants are defined as follows:

$$\alpha = \frac{[H_3L^-]}{[L_f]} = \frac{K_{A1}}{([H^+] + K_{A1})} \qquad (5)$$

and

$$\beta = \frac{[M^{3+}]}{[M_f]} = \frac{1}{\left(1 + \frac{K_{OH1}}{[H^+]} + \frac{3K_{M_3(OH)_4} C_M^2}{[H^+]^4}\right)} \qquad (6)$$

The trimer $M_3(OH)_4^{5+}$ was included in the evaluation of β because its contribution to the total metal concentration exceeds 1% at the lowest of the investigated hydrogen ion concentrations (0.001 M). The plot of $K_{1app}/\alpha\beta$ versus $1/[H^+]$, shown in Figure 4A, is linear, with intercept K_{MH3L} and slope $K_{MH2L} \times K_{OH1}$. The values of the individual equilibrium constants are reported in Table 1.

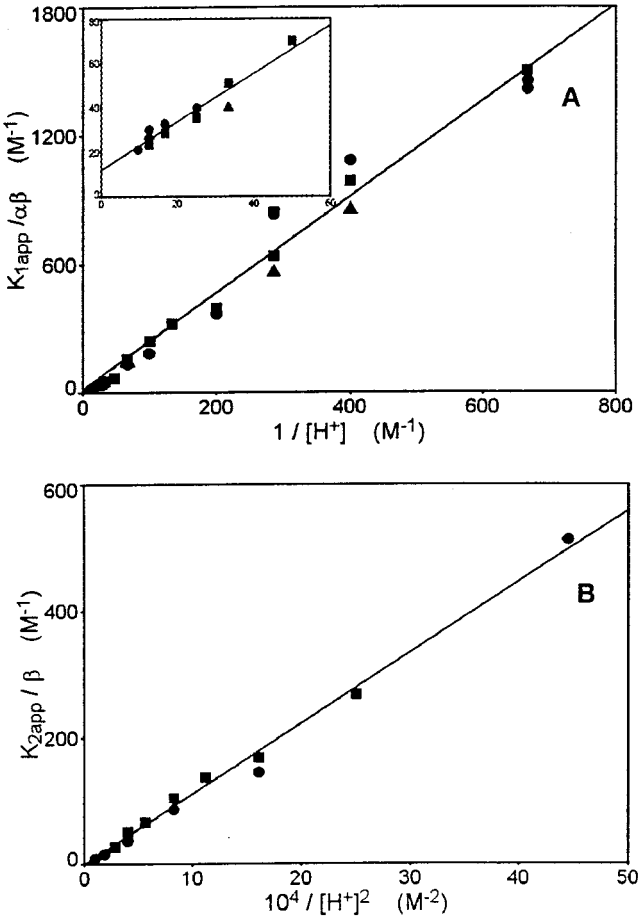

Figure 4. Equilibria of the indium(III)-PCV system at $I = 0.2$ M, and $T = 25$ °C. (A) Plot of $K_{1app}/\alpha\beta$ vs $1/[H^+]$. Data points are from spectrophotometry (●), kinetics (■), and amplitudes (▲). The insert shows that the intercept is positive. (B) Plot of K_{2app}/β versus $1/[H^+]^2$. Data points are from spectrophotometry (●) and kinetics (■).

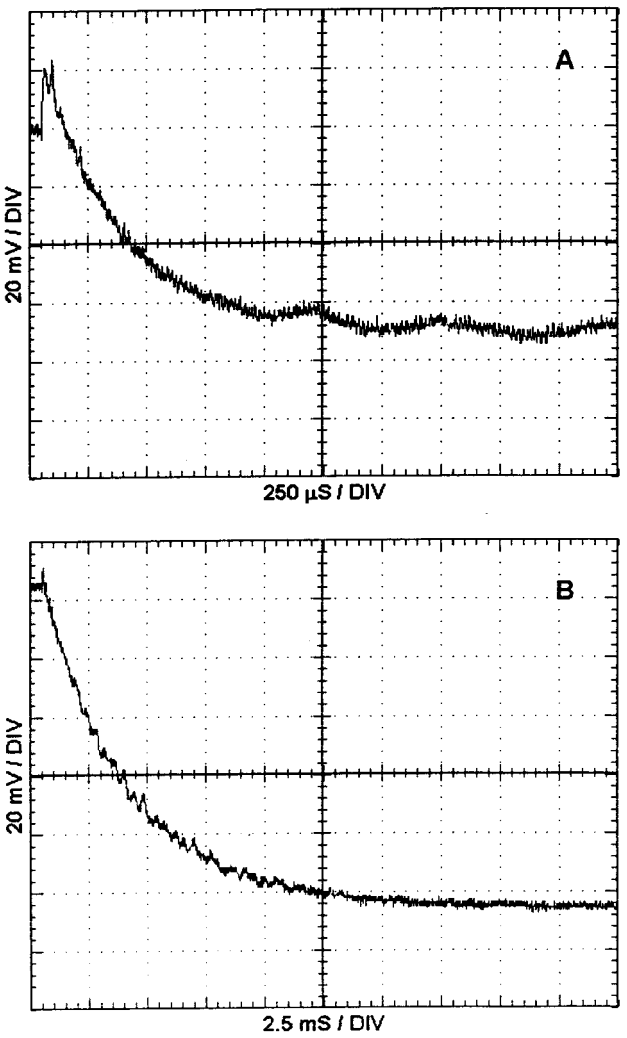

Figure 5. Kinetics of the indium(III)-PCV system at $I = 0.2$ M and $T = 25$ °C. The temperature-jump signals were detected by (A) laser monitoring at 543 nm ($C_L = 8 \times 10^{-5}$ M, $C_M = 5 \times 10^{-4}$ M, and $[H^+] = 0.0035$ M), and (B) laser monitoring at 633 nm ($C_L = 8 \times 10^{-5}$ M, $C_M = 5 \times 10^{-4}$ M, and $[H^+] = 0.001$ M).

The Dinuclear Complex. Figure 4B shows that the values of K_{2app}/β, derived from spectroscopy and from kinetics are proportional to $[H^+]^{-2}$. This kind of dependence is appropriately described by eq 7 and indicates that the binding of the second metal ion to the mononuclear complex occurs with expulsion of two protons:

$$\frac{K_{2app}}{\beta} = \frac{K'_{M_2L}}{[H^+]^2} \tag{7}$$

The slope of the plot provides the value of K'_{M2L}, the equilibrium constant of the reaction $M^{3+} + MH_2L^+ \leftrightarrow M_2L^{2+} + 2H^+$ (see Table 1).

Kinetics. The temperature-jump curves display two measurable relaxation effects that, being well separated on the time scale (see Figure 5), could be analyzed independently. The fastest relaxation (shown in Figure 5A), with relaxation time τ_1, should be associated with the apparent reaction 1, whereas the slowest relaxation (shown in Figure 5B), with relaxation time τ_2, should be associated with a normal mode of reaction arising from a suitable combination of reaction 2 and reaction 1. For $[H^+] \geq 0.015$ M, only the effect depending on reaction 1 was observed at any of the employed metal ion concentrations.

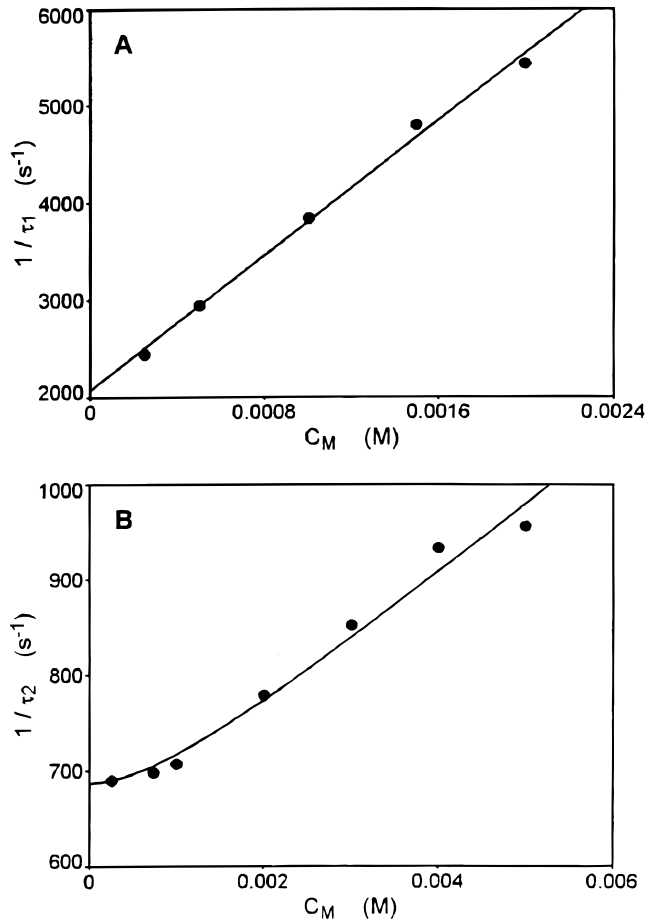

Figure 6. Concentration dependence of the reciprocal relaxation times for the indium(III)-PCV system ($[H^+] = 0.0025$ M, $I = 0.2$ M, and $T = 25$ °C). (A) Plot of $1/\tau_1$ versus C_M, with the fitted line based on eq 6 in the text. (B) Plot of $1/\tau_2$ versus C_M, with the fitted line based on eq 7 in the text.

Given that all the experiments were performed under pseudo-first-order conditions ($C_M \gg C_L$), the concentration dependencies of the relaxation times take the following simple forms:

$$\frac{1}{\tau_1} = k_{1f}C_M + k_{1d} \tag{8}$$

$$\frac{1}{\tau_2} = \frac{K_{1app}k_{2f}C_M^2}{(1 + K_{1app}C_M)} + k_{2d} \tag{9}$$

It should be noticed that the two chemical relaxations are sufficiently separated on the time scale to allow reaction 1 to be considered as a fast preequilibrium; this feature enables us to account for the contribution of reaction 1 to the second relaxation simply by introducing K_{1app} in eq 9. The rate constants of the apparent reaction 1 in the forward and reverse directions are denoted, respectively, k_{1f} and k_{1d}, whereas k_{2f} and k_{2d} indicate the same respective rate constants of the apparent reaction 2. Figure 6 shows the dependence of $1/\tau_1$ and $1/\tau_2$ on C_M. The continuous lines are calculated according to eq 8 and eq 9, respectively.

The Mononuclear Complex. The experiments were performed at $\lambda = 543$ nm, where the change of transmittance of the "red" mononuclear complex is optimal, by using a 0.5 mW He−Ne laser. Plots such as that of Figure 6A drawn for different acidities have shown that both k_{1f} and k_{1d} depend on $[H^+]$. The values of k_{1f}/k_{1d} are in good agreement with the values of K_{1app}

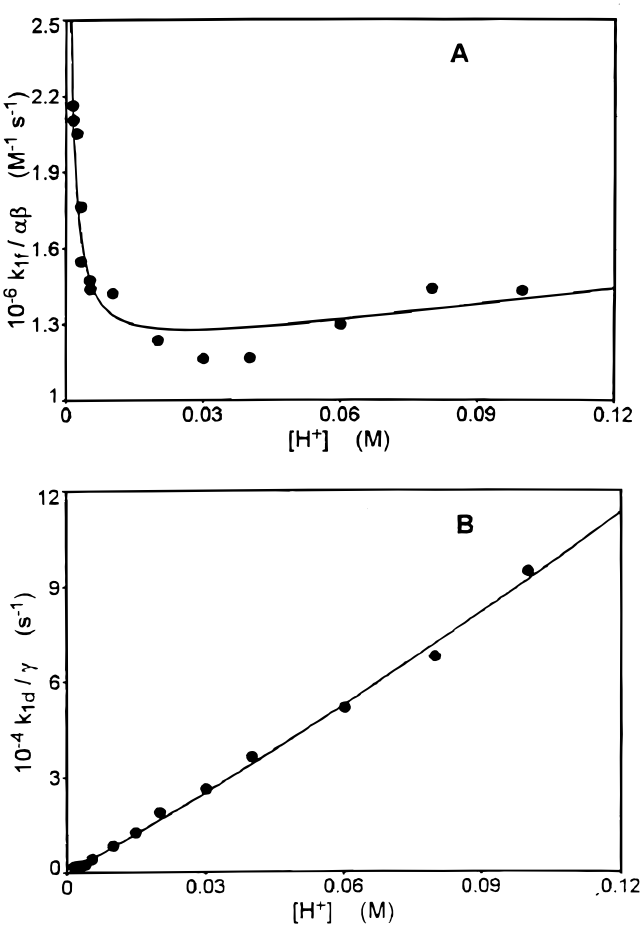

Figure 7. Analysis of the fast relaxation for the indium(III)-PCV system at $I = 0.2$ M and $T = 25$ °C. (A) Plot of $k_{1f}/\alpha\beta$ versus $[H^+]$, with the fitted line based on eq 8 in the text. (B) Plot of k_{1d}/γ versus $[H^+]$, with the fitted line based on eq 9 in the text.

measured by spectophotometry (see Figure 4A). Assuming that all the proton-transfer steps included in the reaction scheme are faster than the complexation steps, the relationships between the apparent and the individual rate constants could be derived in the forms:

$$k_{1f} = \left(\frac{k_3 K_{OH1}}{[H^+]} + k_2 + \frac{k_1[H^+]}{K_{A1}}\right)\alpha\beta \qquad (10)$$

$$k_{1d} = \left(k_{-3} + \frac{k_{-2}[H^+]}{K_{C2}} + \frac{k_{-1}[H^+]^2}{K_{C1}K_{C2}}\right)\gamma \qquad (11)$$

where $\gamma = 1/([H^+]^2/K_{C1}K_{C2} + [H^+]/K_{C2} + 1)$. Because $K_{C1} \gg [H^+]$, the values of γ were calculated by using $\gamma = K_{C2}/([H^+] + K_{C2})$. The rate parameters k_1, k_2, and k_3 were evaluated by applying a nonlinear least-squares fitting to eq 10. A similar procedure was applied to eq 11 to obtain the relevant rate parameters. Figure 7A shows the experimental and the calculated trends. The values of the reaction parameters are collected in Table 1. In principle, the rate parameters are not unambiguously determined because, due to proton ambiguity, step II could be replaced by the kinetically indistinguishable step V.

$$MOH^{2+} + H_4L \rightleftharpoons MH_3L^{2+} + H_2O \qquad (V)$$

In such a case, the forward rate constant of step V, let us call it k'_2, would be $k'_2 = k_2K_{A1}/K_{OH1} = 2.3 \times 10^{10}$ M^{-1} s^{-1}. This value is twice the value of the encounter rate for a diffusion-controlled reaction involving a neutral species. Therefore, step V was dropped out of the reaction scheme. All possible reaction steps involving the ligand in the forms H_2L^{2-}, HL^{3-}, and L^{4-} have not been considered here because, at the acidity of the experiments, the concentrations of these species are extremely low (cf. the pK_A values in Table 1). Similar considerations apply to all possible steps involving the metal in the form $M(OH)_2^+$.

Reaction Parameters. The apparent activation parameters of reaction 1 have been derived from rate measurements performed at five different temperatures ranging between 15 and 35 °C. For $[H^+] = 0.03$ M, the apparent activation enthalpies are $\Delta H_{1f}^{\ddagger} = 25.3$ kJ mol^{-1} and $\Delta H_{1d}^{\ddagger} = 13.4$ kJ mol^{-1}, from which the activation entropies have been estimated as $\Delta S_{1f}^{\ddagger} = -6.2$ J mol^{-1} K^{-1} and $\Delta S_{1d}^{\ddagger} = -57$ J mol^{-1} K^{-1}. The activation enthalpies difference yields the reaction enthalpy as $\Delta H_1^0 = 11.9$ kJ mol^{-1}, whereas the van't Hoff analysis of K_{1app} yields $\Delta H_1^0 = 11.3$ kJ mol^{-1}. Furthermore, ΔH_1^0 and ΔH_2^0 were evaluated by the amplitude analysis described below.

Salt Effects. The influence of the addition of sodium and magnesium perchlorates on k_{1f} and k_{1d} was investigated at $[H^+] = 0.015$ M. The value of k_{1f} decreases whereas k_{1d} increases, by increasing the ionic strength. The salt effect is more modest in the reverse than in the forward direction. These observations are in agreement with the charge values of the species involved in step II, which are prevailing at the working $[H^+]$. Actually, under these conditions, $k_{1f} \approx k_2$ and $k_{1d} \approx K_{C2}^{-1}\, k_{-2}$. The salt effects were analyzed according to the equation $\log k = \log k_0 + 1.02\, z_M z_L\, I^{1/2}/(1 + I^{1/2}) + BI$, which, for $z_M z_L = -3$, yields $\log k_{1f}^0 = 6.93$ and $B = 1.3$ (Figure 8A), whereas for $z_M z_L = 1$, yields $\log k_{1d}^0 = 5.75$ and $B = -0.26$ (Figure 8B). Considering that the interaction between M^{3+} and H_3L^- leads, as a primary reaction act, to formation of an outer-sphere ion pair,[13] the salt effect on k_{1f} should reflect the ionic strength dependence of the stability constant of the outer complex. On the other hand, the positive effect on the reverse reaction should mainly reflect the ionic strength dependence of the acid dissociation constant K_{C2}. No substantial differences could be found between sodium and magnesium.

Figure 9 shows the result of a series of experiments performed with different concentrations of sodium sulfate at constant ionic strength. The reduction of $1/\tau_1$ is too large to be ascribed to a simple salt effect. This view is also supported by the (not shown) large changes of the relaxation amplitudes and by the large variations of absorbance observed in equilibrium measurements in the presence of sulfate. Ascribing the rate reduction to the binding of sulfate to the metal, the results could be rationalized by coupling reaction 1 with reaction 12

$$M_f + SO_{4f} \rightleftharpoons MSO_{4T} \qquad (12)$$

which, for $C_{Na2SO4} \gg C_M \gg C_L$, equilibrates much faster[14] than reaction 1. Under these circumstances, the expression for the relaxation time becomes

$$\frac{1}{\tau_1} = \frac{k_{1f}C_M}{(1 + KC_{Na_2SO_4})} + k_{1d} \qquad (13)$$

where K is the equilibrium constant of reaction 12. The analysis of the data according to eq 13 yields $K = (1.5 \pm 0.6) \times 10^2$ M^{-1}. By using for the second dissociation constant of H_2SO_4 at $I = 0.2$ M the value $K_{A2} = 3.2 \times 10^{-2}$ M,[15] the stability constant of the complex $InSO_4^+$ is obtained as $K(InSO_4^+) = K \times (1 + [H^+]/K_{A2}) = 220$ M^{-1}. This value is in good agreement with the value of 166 M^{-1} obtained by reducing our ionic strength to the literature value.[15]

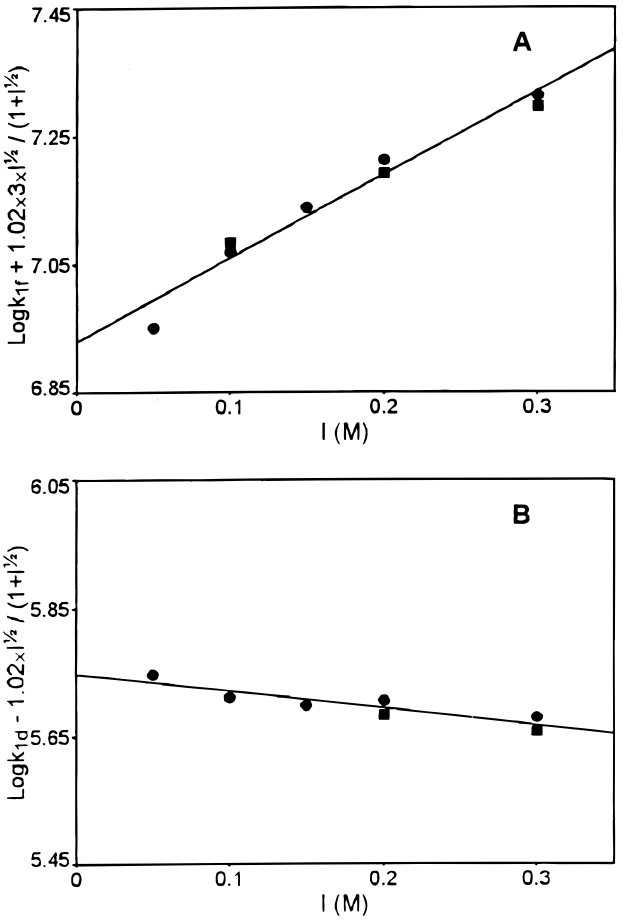

Figure 8. Salt effect on the indium(III)-PCV system at $[H^+] = 0.015$ M and $T = 25$ °C: (A) ionic strength effect on the rate constant of complex formation; (B) ionic strength effect on the rate constant of complex dissociation. The fitted lines are based on ref 12.

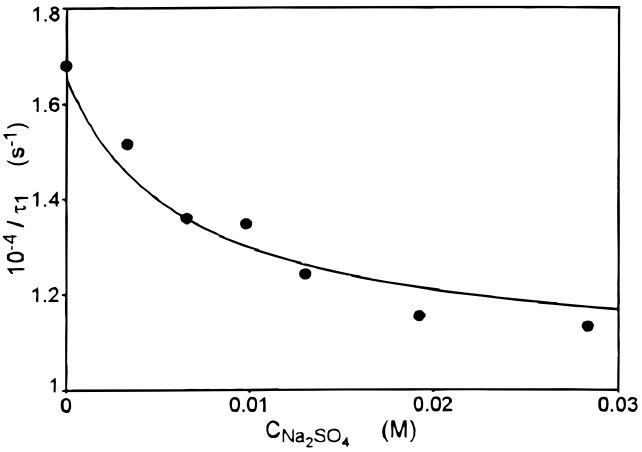

Figure 9. The indium(III)-PCV system at $I = 0.3$ M, $T = 25$ °C, $C_M = 3.3 \times 10^{-3}$ M, and $[H^+] = 0.015$ M. The effect of the addition of sodium sulfate on the fast relaxation time. The fitted line is based on eq 13 in the text.

The Dinuclear Complex. The relaxation effect associated with the "blue" dinuclear complex was measured at $[H^+] < 0.015$ M. Because at 543 nm the amplitudes of this relaxation are very small, particularly at low metal ion concentrations, it was found convenient to use as a light source a 5 mW laser emitting at 633 nm. The dependence of the reciprocal relaxation time, $1/\tau_2$, on C_M is shown in Figure 6B for $[H^+] = 2.5 \times 10^{-3}$ M. The trend is initially parabolic and tends to become linear for high values of C_M. The reaction constants k_{2f} and k_{2d} were evaluated

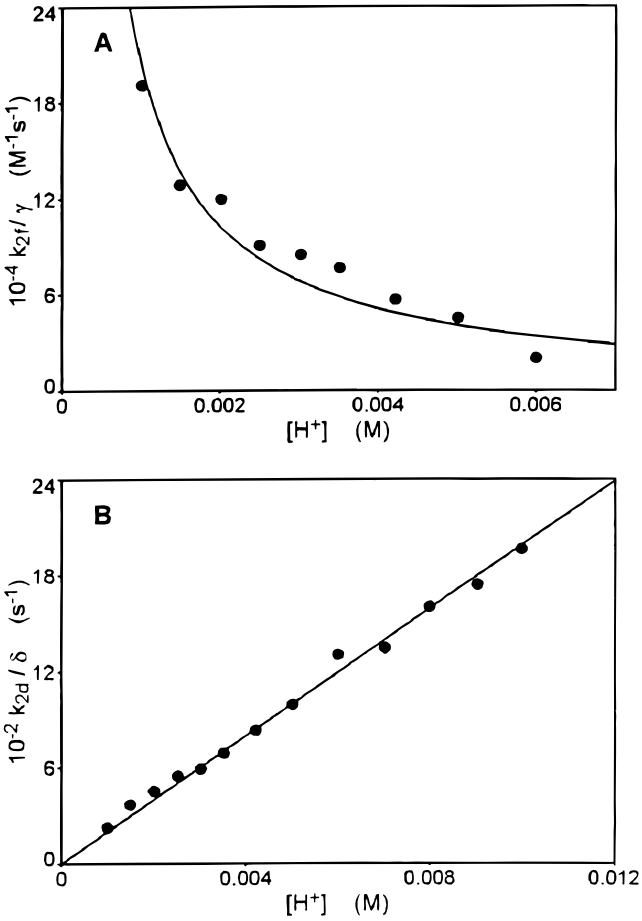

Figure 10. Analysis of slow relaxation for the indium(III)-PCV system at $I = 0.2$ M and $T = 25$ °C. (A**)** Plot of k_{2f}/γ versus $[H^+]$, with the fitted line based on eq 14 in the text. (B**)** Plot of k_{2d}/δ versus $[H^+]$, with the fitted line based on eq 15 in the text.

according to eq 9 by a fitting procedure where K_{1app} was introduced as a know value. For $[H^+]$ values between 0.006 and 0.01 M, plots like that in Figure 6B tend to give straight lines parallel to the x axis, which make it impossible to measure k_{2f}. However, the values of k_{2d} could still be evaluated from the intercepts on the y axis. Figure 10A shows that k_{2f}/γ decreases continuously by increasing the acidity level, whereas Figure 10B shows that k_{2d} is directly proportional to $[H^+]$. These observations indicate that only a single path that we identify with step IV of the reaction scheme is operative in the formation and dissociation of the dinuclear complex. The analysis of the equilibria does not provide evidence for the presence of sizable amounts of MHL in the investigated range of pH values. Under these circumstances the dependence of k_{2f} on $[H^+]$ is given by eq 14

$$k_{2f} = \frac{K_{C_3} k_4}{[H^+]}\gamma \tag{14}$$

Concerning the reverse step, because no evidence has been found for noticeable concentrations of M_2HL, one can write

$$k_{2d} = \frac{k_{-4}[H^+]}{K_{D_4}}\delta \tag{15}$$

where $\delta = 1/(1 + [H^+]/K_{D4}) \simeq 1$ is the molar fraction of M_2L. The analysis of the plots of Figures 10A and 10B yield

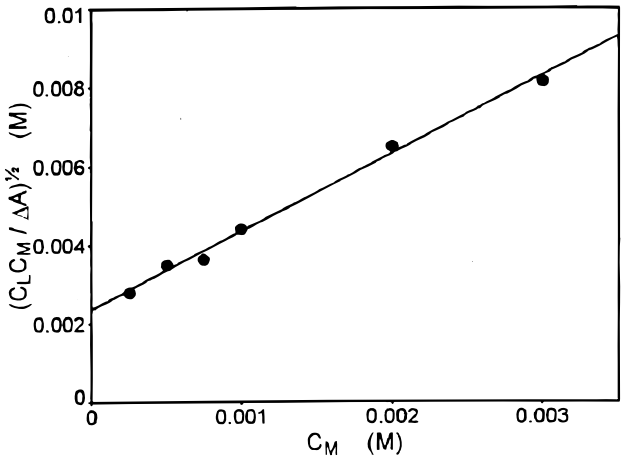

Figure 11. The indium(III)-PCV system at $I = 0.2$ M and $T = 25$ °C. Amplitude analysis of the fast relaxation effect. The fitted line is based on eq 18 in the text.

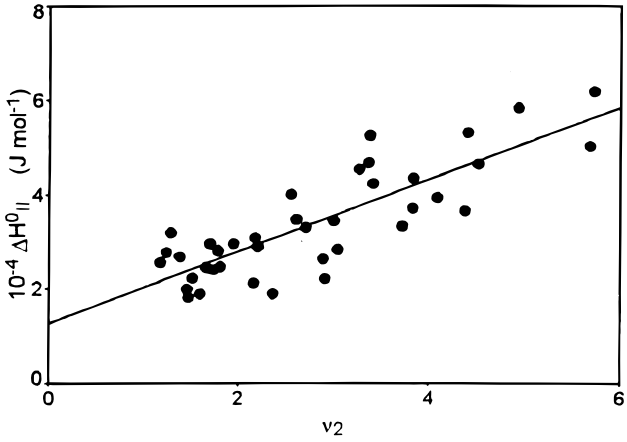

Figure 12. The indium(III)-PCV system at $I = 0.2$ M and $T = 25$ °C. Amplitude analysis of the slow relaxation effect. The fitted line is based on $\Delta H_{II}^0 = \Delta H_1^0 + \nu_2\,\Delta H_2^0$.

respectively the reaction parameters $K_{C3}\,k_4$ and $K_{D4}^{-1}\,k_{-4}$ whose values are reported in Table 1.

Amplitude Analysis. The chemical relaxation theory[16] allows the analysis of a system of coupled reactions to be performed in terms of normal modes of reaction, otherwise denoted as "normal reactions", which are suitable linear combinations of the thermodynamically independent reactions present in the system.[17] In the case of spectrophotometric signal detection, the amplitude of the k^{th} normal mode is given by the equation

$$\delta A_k^0 = \frac{\Delta\epsilon_k \Gamma_k \Delta H_k^0 \delta T}{RT^2} \qquad (16)$$

where $\Delta\varepsilon_k$ is the extinction coefficient difference between products and reactants appearing in the k^{th} normal reaction, Γ_k is an amplitude factor containing the equilibrium constant of the k^{th} normal reaction, ΔH_k^0 is the related reaction enthalpy, and δT is the jump of temperature. The linear combination leading to the normal reactions is conveniently obtained by adding ν times reaction 2 to reaction 1. The resulting normal reactions read[18]

$$(1 + \nu_k)\mathrm{M} + \mathrm{L} \rightleftharpoons (1 - \nu_k)\mathrm{ML} + \nu_k \mathrm{M_2L} \qquad (17)$$

where[17] $\nu_k = -(b_{11} - 1/\tau_k)/b_{12}$. In turn $b_{11} = k_{1f}\,(C_M + 1/K_{1app})$ and $b_{12} = -(k_{1f}/K_{1app})$.

The first normal reaction ($k = 1$) equilibrates much faster than the second. Hence, it turns out that $b_{11} = 1/\tau_1$ and, as a consequence, $\nu_1 = 0$, which means that the first normal reaction coincides with reaction 1. Its amplitude factor is[18] $\Gamma_I = 1/(1/C_M + 1/[L_f] + 1/[ML_T])$. Neglecting $1/C_M$ in the sum and writing Γ_I as a function of analytical concentrations, eq 16 is reduced to[18]

$$\left(\frac{C_L C_M}{\delta A_1^0}\right)^{1/2} = \frac{1}{B} + \left(\frac{K_{1app}}{B}\right) C_M \qquad (18)$$

where $B = (l\,\Delta\varepsilon_1\,\Delta H_1^0 K_{1app}\delta T/RT^2)^{1/2}$. Figure 11 shows an example of the amplitude analysis according to eq 18. The values of K_{1app} obtained at different acidities from plots as that of Figure 11 agree with the corresponding values derived from static measurements and from kinetics (see Figure 4A). The ΔH_1^0 values obtained from the intercepts of 10 plots at different acidities ($[H^+] = 0.015$ to 0.08 M) and temperature (15 to 35 °C) are close together and do not display any appreciable trend, the mean value being $\Delta H_1^0 = 12.0 \pm 0.9$ kJ mol^{-1}.

Concerning the second normal reaction ($k = 2$), the normal-mode analysis yields $\nu_2 = -(b_{11} - 1/\tau_2)/b_{12} \approx -b_{11}/b_{12} = 1 + K_{1app}C_M$, because $1/\tau_2 \ll b_{11}$. The amplitude factor,[17] $\Gamma_{II} = 1/\{(1 + \nu_2)^2/C_M + 1/[L_f] + (1 - \nu_2)^2/[ML_T] + \nu_2^2/[M_2L_T]\}$, was evaluated for each sample. Being the second normal reaction made by reaction 1 plus ν_2 times reaction 2, it turns out that $\Delta\epsilon_{II} = \Delta\epsilon_1 + \nu_2\,\Delta\epsilon_2$ and $\Delta H_{II}^0 = \Delta H_1^0 + \nu_2\,\Delta H_2^0$. Therefore, the reaction enthalpies of reactions 1 and 2 could be simultaneously determined by deriving ΔH_{II}^0 from eq 16 and then plotting this quantity as a function of ν_2. This plot is shown in Figure 12 for all the experiments with $[H^+] \leq 0.01$ M. The intercept and slope yield, respectively, $\Delta H_1^0 = 12.6 \pm 2.4$ kJ mol^{-1} and $\Delta H_2^0 = 7.6 \pm 0.8$ kJ mol^{-1}.

Discussion

Equilibria. Figure 4 shows that equilibrium constants derived from the dynamic method are as accurate as those derived from spectrophotometry. However, the dynamic method offers some advantages over the static one. First, the equilibrium constants could be derived from relaxation times and, independently, from amplitudes. Second, the total change of absorbance contains an instantaneous contribution due to the thermal expansion of the sample that could be resolved in time from the effect due to chemical relaxation. In contrast, static measurements at different temperatures provide signals that, due to the overlap of physical and chemical effects, could in principle lead to erroneous results.[19] Third, the reaction enthalpies of the individual steps can be easily obtained under dilution conditions such that the calorimetric measurements could give unreliable responses (in our experiments, C_L never exceeded 8×10^{-5} M). Finally, it should be noticed that in classical spectrophotometry, signal amplification cannot forward any improvement of resolution, whereas in the dynamic method, it can enhance the response to levels that could provide a sensitive measure of the equilibrium constants.[19] The accuracy of the measurements is limited by the noise associated with the amplification of the small transient signals, which are displayed by highly formed systems. This noise should be minimized, which could be appropriately done by our device with laser sources,[10] where the signal-to-noise ratio is ~1 order of magnitude better than that of the commercial instrumentation.

A comparison between In(III)−PCV and the previously investigated Ga(III)−PCV system,[4] shows that in the latter, no noticeable amounts of the triprotonated species MH_3L^{2+} could

TABLE 2: Comparison of Rate Constants for Substitution at In^{3+} (k_1) and at $InOH^{2+}$ (k_2)

ligand	I (M)	k_1 ($M^{-1}\,s^{-1}$)	k_1/K_{OS} (s^{-1})	k_2 ($M^{-1}\,s^{-1}$)	k_2/K_{OS} (s^{-1})	ref
$Hferron^+$	0.2	1.1×10^3	4.1×10^4			6
$Ferron^0$	0.2	9.7×10^4	3.1×10^5	1.2×10^7	3.8×10^7	6
H_4L^0	0.2	1.6×10^6	5.1×10^5			this work
H_3L^-	0.2	1.2×10^6	3.2×10^5	4.4×10^7	2.7×10^7	this work
$Murexide^-$	0.1	6.0×10^5	1.1×10^5			25
SOX^- [a]	0.1	2.8×10^5	5.3×10^4			26
SO_4^{2-}	0	2.6×10^5	1.6×10^2	2.5×10^7	2.6×10^5	14
H_2O			2.0×10^4			21

[a] Semixylenol orange.

be found despite the higher hydrogen ion concentration of the experiments. The presence of this species in the In(III)−PVC system could be ascribed to the larger ionic radius of In^{3+} and to the consequent reduction of charge density on the metal ion. An example of connection between ionic radius and stability of the protonated complexes is provided by the lanthanides−malonate system.[20] Concerning the dinuclear species, we ascribe the absence of noticeable amounts of $M_2H_2L^{4+}$ or $M_2H_3L^{5+}$ to their too high charges, which facilitate the expulsion of protons. The resulting M_2L^{2+} ion is stabilized because of its reduced charge and the chelation effect.

Kinetics. The hydrolyzed form $InOH^{2+}$ shows enhanced reactivity, as is usual in complex formation of tervalent metal ions [V(III) and Ti(III) excluded].[3] Whatever the mechanism of complex formation should be, the electrostatic interaction between the reaction partners must be accounted for in deriving the rate constants of the individual complexation steps from the observed relaxation times. This requirement could be met by dividing the observed second-order rate constants, k, by the ion-pair formation constant, K_{os}. This operation will provide a suitable tool for correcting the reaction rate for charge and ionic strength effects, although some uncertainty arises from the arbitrary choice of the charge distance in the ion pair.

Table 2 shows the results for the available data in water solution. All values of k/K_{os} are higher than those found for similar reactions involving gallium and aluminum, which is in agreement with the reactivity sequence In(III) > Ga(III) > Al(III). With the exclusion of the results for the In(III)−SO_4^{2-} system (derived from extrapolations to $I = 0$ M of data collected at high and variable ionic strength), the values of k/K_{os} appear to be rather similar both for In^{3+} and $InOH^{2+}$. Actually, no definite trend emerges that would connect the rate constants with nucleophilic properties of the ligand, such as basicity or polarizability. If present, this trend could provide indication for an interchange associative mode of activation. Very recent O^{17} nuclear magnetic resonance (NMR) measurements,[8] made by the terbium shift reagent method, led to the conclusion that the rate of water exchange at In^{3+} should be $> 10^7\ s^{-1}$, three orders of magnitude higher than the commonly accepted value of $4 \times 10^4\ s^{-1}$ quoted by Glass et al.[21] The large uncertainty in the value of this important parameter makes it rather hard to include the Eigen criterion[22] among the tests to be done to elucidate the mechanism of complex formation of In(III). The determination of activation volumes for both solvent exchange and complex formation would provide a valuable aid in the assignment of the reaction mechanism. Unfortunately the $\Delta V^{\ddagger}$ value for water exchange at $In(H_2O)_6^{3+}$ is not yet available. However, we know[23] that the activation volumes for DMSO replacement by Hitp (a Tropolone derivative) in DMSO solvent for Al^{3+}, Ga^{3+}, and In^{3+} are, respectively, +12.2, +10.6, and $-0.1\ cm^3\ mol^{-1}$. Moreover, by considerations based on the bond making and bond breaking argument, Kowall et al.[8] estimated a value of $-5.2\ cm^3\ mol^{-1}$ for $\Delta V^{\ddagger}$ of water exchange at In^{3+}, whereas the values of $\Delta V^{\ddagger}$ for Al^{3+} and Ga^{3+}, whose dissociative mechanism of water exchange is now widely accepted, are, respectively, +5.7 and $+5.0\ cm^3\ mol^{-1}$. The slightly negative activation volumes for both water exchange and Hipt complexation at In^{3+} seem to indicate that this ion could react via a transition state where both the solvent and the incoming ligand are loosely coordinated, which once again is in agreement with the large radius of the In^{3+} ion. If the complex formation and solvent exchange process undergoes the same mechanism, our slightly negative value of $\Delta S^{\ddagger}$ for the reaction between In^{3+} and H_3L^- seems to support the just presented argument. In conclusion, no definite evidence in favor of an I_d or I_a mode of activation could be found for complexation of In(III) on the basis of the presently available results. Certainly, systematic studies with ligands of different basicity but with similar structure and relaxation measurements at high pressures are highly desiderable in this context.

References and Notes

(1) Hayes, R. L.; Hubner, K. F. In *Metal Ions in Biological Systems*; Sigel, H., Ed.; Dekker: New York, 1983; Vol 16, p 279.

(2) Baes, C. F., Jr.; Mesmer, R. E. *The Hydrolysis of Cations*; John Wiley & Sons: New York, 1976; p 313.

(3) Burgess, J. *Metal Ions in Solution*; Ellis Horwood: Chichester, 1978; p 371.

(4) Corigli, R.; Secco, F.; Venturini, M. *Inorg. Chem.* **1979**, *18*, 3184.

(5) Corigli, R.; Secco, F.; Venturini, M. *Inorg. Chem.* **1982,** *21*, 2992.

(6) Perlmutter-Hayman, B.; Secco, F.; Venturini, M. *J. Chem. Soc., Dalton Trans.* **1982**, 1945.

(7) Perlmutter-Hayman, B.; Secco, F.; Venturini, M. *Inorg. Chem.* **1985**, *24*, 3828.

(8) Kowall, Th.; Caravan, P.; Bourgeois, H.; Helm, L.; Rotzinger, F. P.; Merbach, A. E. *J. Am. Chem. Soc.* **1998**, *120*, 6569.

(9) Savvin, S. B. *Crit. Rev. Anal. Chem.* **1979**, *8*, 55.

(10) Citi, M.; Festa, C.; Secco, F.; Venturini, M. *Instrum. Sci. Technol.* **1995**, *23*, 191.

(11) Provencher, S. W. *J. Chem. Phys.* **1976**, *64*, 2772.

(12) Guggenheim, E. A.; Prue, J. E. *Physicochemical Calculations*; North-Holland: Amsterdam, 1956; p 466.

(13) Fuoss, R. M. *J. Am. Chem. Soc.* **1958**, *80*, 5059.

(14) Miceli, J.; Stuehr, J. *J. Am. Chem. Soc.* **1968**, *90*, 6967.

(15) *Stability Constants*, Special Publication No. 17; Sillen, L.; Martell, A. Ed.; The Chemical Society: London, 1964.

(16) Eigen, M.; De Maeyer, L. In *Techniques of Chemistry*; Hammes, G. G., Ed.; John Wiley & Sons: New York, 1974; Vol VI, p 63.

(17) Maggini, R.; Secco, F.; Venturini, M. *J. Phys. Chem.* **1997**, *101*, 5666.

(18) Citi, M.; Secco, F.; Venturini, M. *J. Phys. Chem.* **1988**, *92*, 6399.

(19) Winkler-Ostwatitsch, R.; Eigen, M. *Angew. Chem., Int. Ed. Engl.* **1979**, *18*, 20.

(20) Martell, A. E.; Smith R. M. In *Critical Stability Constants*; Plenum: New York, 1977; Vol 3, p 95.

(21) Glass, G. E.; Schwabacher, W. B.; Tobias, R. S. *Inorg. Chem.* **1968**, *7*, 2471.

(22) Eigen, M.; Tamm; K. *Z. Elektrochem.* **1962**, *66*, 93.

(23) Ishihara, K.; Funahashi, S.; Tanaka, M. *Inorg. Chem.* **1986**, *25*, 2898.

(24) Ryba, O.; Cifka, J.; Malàt, M.; Suk, V. *Collect. Czech. Chem. Commun.* **1956**, *21*, 349.

(25) Kawai, Y.; Imamura, T.; Fujimoto, M. *Bull. Chem. Soc. Jpn.* **1975**, *48*, 3142; Ohtani, Y.; Yagihashi, S.; Fujimoto, M. *Bull. Chem. Soc. Jpn.* **1977**, *50*, 1345.

(26) Kawai, Y.; Takahashi, T.; Hayashi, K.; Imamura, T.; Nakayama, H.; Fujimoto, M. *Bull. Chem. Soc. Jpn.* **1972**, *45*, 1417.